



Precision measurement of the mass and lifetime of the Ξ_b^- baryon

The LHCb collaboration[†]

Abstract

We report on measurements of the mass and lifetime of the Ξ_b^- baryon using about 1800 Ξ_b^- decays reconstructed in a proton-proton collision data set corresponding to an integrated luminosity of 3.0 fb^{-1} collected by the LHCb experiment. The decays are reconstructed in the $\Xi_b^- \rightarrow \Xi_c^0 \pi^-$, $\Xi_c^0 \rightarrow p K^- K^- \pi^+$ channel and the mass and lifetime are measured using the $\Lambda_b^0 \rightarrow \Lambda_c^+ \pi^-$ mode as a reference. We measure

$$M(\Xi_b^-) - M(\Lambda_b^0) = 178.36 \pm 0.46 \pm 0.16 \text{ MeV}/c^2,$$

$$\frac{\tau_{\Xi_b^-}}{\tau_{\Lambda_b^0}} = 1.089 \pm 0.026 \pm 0.011,$$

where the uncertainties are statistical and systematic, respectively. These results lead to a factor of two better precision on the Ξ_b^- mass and lifetime compared to previous best measurements, and are consistent with theoretical expectations.

Published in Physical Review Letters

© CERN on behalf of the LHCb collaboration, license CC-BY-4.0.

[†]Authors are listed at the end of this Letter.

Over the last two decades, beauty mesons have been studied in detail. Various theoretical approaches allow one to relate measured decay rates to Standard Model parameters. One of the most predictive tools is the heavy quark expansion (HQE) [1–8], which describes the decay rates of beauty hadrons through an expansion in powers of Λ_{QCD}/m_b , where Λ_{QCD} is the energy scale at which the strong-interaction coupling becomes large, and m_b is the b -quark mass. In addition to the total b -hadron decay widths, HQE can be used to calculate b -hadron parameters required for the measurement of coupling strengths between quarks in charged-current interactions, which in turn provides constraints on physics beyond the Standard Model.

A stringent test of HQE is to confront its predictions for lifetimes, *i.e.*, the inverse of the corresponding decay widths, with precision measurements. The lifetimes of the B^0 and B^+ mesons are measured to a precision of about 0.5% [9], the B_s^0 meson to 1% [9, 10], and the Λ_b^0 baryon to 0.7% [9], and their values are in agreement with HQE predictions [11].

Another interesting test is to compare the measured lifetime ratio $\tau(\Xi_b^-)/\tau(\Xi_b^0)$ to HQE predictions. Since penguin contraction terms cancel in this ratio [12], a more precise prediction is possible compared to $\tau(\Lambda_b^0)/\tau(B^0)$. One prediction leads to $\tau(\Xi_b^-)/\tau(\Xi_b^0) = 1.05 \pm 0.07$ [12], where the dominant uncertainties are related to matrix elements that are calculable using lattice quantum chromodynamics (QCD) [13]. A phenomenological analysis of the relevant matrix elements using charm baryon lifetimes leads to a prediction of $1/\tau(\Lambda_b^0) - 1/\tau(\Xi_b^-) = 0.11 \pm 0.03 \text{ ps}^{-1}$ [14], or $\tau(\Xi_b^-)/\tau(\Lambda_b^0) = 1.19_{-0.06}^{+0.07}$. Recently, the first measurement of the lifetime ratio $\tau(\Xi_b^0)/\tau(\Lambda_b^0)$ was made, yielding $\tau(\Xi_b^0)/\tau(\Lambda_b^0) = 1.006 \pm 0.018 \pm 0.010$ [15]. Previous Ξ_b^- lifetime measurements, which used $\Xi_b^- \rightarrow J/\psi \Xi^-$ decays, led to values of $1.55_{-0.09}^{+0.10} \pm 0.03 \text{ ps}$ [16] and $1.32 \pm 0.14 \pm 0.02 \text{ ps}$ [17]. The weighted average of these two results, along with the recent Ξ_b^0 lifetime measurement [15], yields $\tau(\Xi_b^-)/\tau(\Xi_b^0) = 1.00 \pm 0.06$. Improved experimental and theoretical precision of the Ξ_b^- lifetime will allow for a more stringent test of the HQE prediction.

Measurements of b -baryon masses and isospin splittings provide information on the interquark potential. A number of QCD-inspired models predict the Ξ_b^0 and Ξ_b^- masses, or their average, which range from approximately $5780 \text{ MeV}/c^2$ to $5900 \text{ MeV}/c^2$ [18–27]. More accurate predictions exist for the $\Xi_b^- - \Xi_b^0$ mass splitting, estimated to be $6.24 \pm 0.21 \text{ MeV}/c^2$ or $6.4 \pm 1.6 \text{ MeV}/c^2$ when extrapolating from the measured isospin splitting $M(\Xi^-) - M(\Xi^0)$ or $M(\Xi_c^0) - M(\Xi_c^+)$, respectively [22]. The Ξ_b^- mass is currently known to a precision of $1.0 \text{ MeV}/c^2$ [28], which is a factor of three less precise than that of the Ξ_b^0 baryon [15].

In this Letter, we report improved measurements of the mass and lifetime of the Ξ_b^- baryon using about 1800 $\Xi_b^- \rightarrow \Xi_c^0 \pi^-$, $\Xi_c^0 \rightarrow pK^- K^- \pi^+$ signal decays. The measurements are normalized using the $\Lambda_b^0 \rightarrow \Lambda_c^+ \pi^-$, $\Lambda_c^+ \rightarrow pK^- \pi^+$ decay as a reference. Charge conjugate processes are implied throughout.

The measurements use proton-proton (pp) collision data samples, collected by the LHCb experiment, corresponding to an integrated luminosity of 3.0 fb^{-1} , of which 1.0 fb^{-1} was recorded at a center-of-mass energy of 7 TeV and 2.0 fb^{-1} at 8 TeV. The LHCb detector [29] is a single-arm forward spectrometer covering the pseudorapidity range $2 < \eta < 5$, designed for the study of particles containing b or c quarks. The detector includes a high-precision tracking system, which provides a momentum measurement with

precision of about 0.5% from 2–100 GeV/ c and impact parameter resolution of 20 μm for particles with large transverse momentum (p_{T}). The polarity of the dipole magnet is reversed periodically throughout data-taking to reduce asymmetries in the detection of charged particles. Ring-imaging Cherenkov detectors [30] are used to distinguish charged hadrons. Photon, electron and hadron candidates are identified using a calorimeter system, followed by detectors to identify muons [31].

The trigger [32] consists of a hardware stage, based on information from the calorimeter and muon systems, followed by a software stage, which applies a full event reconstruction [32, 33]. About 57% of the selected X_b events are triggered at the hardware level by one or more of the X_b final-state particles. (Throughout, we use X_b (X_c) to refer to either a Ξ_b^- (Ξ_c^0) or Λ_b^0 (Λ_c^+) baryon.) The remaining 43% are triggered only on other activity in the event. We refer to these two classes of events as triggered on signal (TOS) and triggered independently of signal (TIS). The software trigger requires a two-, three- or four-track secondary vertex with a large scalar p_{T} sum of the particles and a significant displacement from the primary pp interaction vertices (PVs). At least one particle should have $p_{\text{T}} > 1.7 \text{ GeV}/c$ and be inconsistent with coming from any of the PVs. The signal candidates are required to pass a multivariate software trigger selection algorithm [33].

Proton-proton collisions are simulated using PYTHIA [34] with a specific LHCb configuration [35]. Decays of hadronic particles are described by EVTGEN [36], in which final-state radiation is generated using PHOTOS [37]. The interaction of the generated particles with the detector and its response are implemented using the GEANT4 toolkit [38] as described in Ref. [39]. The X_c final states are modeled using a combination of resonant and nonresonant contributions to reproduce the substructures seen in data.

Signal Ξ_b^- (Λ_b^0) candidates are formed by combining in a kinematic fit a $\Xi_c^0 \rightarrow pK^-K^-\pi^+$ ($\Lambda_c^+ \rightarrow pK^-\pi^+$) candidate with a π^- candidate (referred to as the bachelor). The X_b candidate is included in the fit to each PV and is then associated with the one for which the χ^2 increases by the smallest amount. The kinematic fit exploits PV, X_b and X_c decay-vertex constraints to improve the mass resolution. The X_c decay products are each required to have $p_{\text{T}} > 100 \text{ MeV}/c$, and the bachelor pion is required to have $p_{\text{T}} > 500 \text{ MeV}/c$. All final-state particles from the signal candidate are required to have trajectories that are significantly displaced from the PV and to pass particle identification (PID) requirements. The K^- and π^+ PID efficiencies are determined from $D^{*+} \rightarrow D^0\pi^+$, $D^0 \rightarrow K^-\pi^+$ calibration samples, whereas the proton PID efficiency is determined from simulation. The PID efficiencies are reweighted to account for different momentum spectra and track occupancies between the calibration and signal samples. The efficiencies of the PID requirements on the Ξ_c^0 and Λ_c^+ final states are 80% and 86%, respectively. Mass vetoes are used to suppress cross-feeds from misidentified $D_{(s)}^+ \rightarrow K^+K^-\pi^+$, $D^{*+} \rightarrow D^0(K^+K^-\pi^+)$, and $D^+ \rightarrow K^-\pi^+\pi^+$ decays faking $\Lambda_c^+ \rightarrow pK^-\pi^+$ decays, as in Ref. [15]. The difference between the Ξ_c^0 (Λ_c^+) candidate mass and the known value [9] is required to be less than $14 \text{ MeV}/c^2$ ($20 \text{ MeV}/c^2$), which is about 2.5 times the mass resolution.

To improve the signal-to-background ratio, we employ a boosted decision tree (BDT) discriminant [40, 41] built from the same variables used in Ref. [15]. To train the BDT, the kinematic distributions of the signal are modeled using simulated decays. The background is

modeled using signal candidates with X_b invariant mass greater than $300 \text{ MeV}/c^2$ above the signal peak mass. To increase the size of the background sample for the Ξ_b^- BDT training, we also include events in the Ξ_c^0 sideband regions, $20 < |M(pK^-K^-\pi^+) - M(\Xi_c^0)| < 50 \text{ MeV}/c^2$. The BDT requirement is chosen to minimize the expected Ξ_b^- relative yield uncertainty, corresponding to a selection efficiency of 97% (50%) for signal (combinatorial background). The fraction of events with multiple candidates is below 1% (mostly one extra candidate) over the full fit range in both the signal and normalization modes. All candidates are kept.

The invariant mass signal shapes are obtained from simulated $\Xi_b^- \rightarrow \Xi_c^0 \pi^-$ and $\Lambda_b^0 \rightarrow \Lambda_c^+ \pi^-$ decays. They are each modeled by the sum of two Crystal Ball (CB) functions [42] with a common mean as

$$f_{\text{sig}}^{\Lambda_b^0} = f_{\text{low}} \times \text{CB}_-(m_0, \sigma_-, \alpha_-, n) + (1 - f_{\text{low}}) \times \text{CB}_+(m_0, \sigma_+, \alpha_+, n) \quad (1)$$

$$f_{\text{sig}}^{\Xi_b^-} = f_{\text{low}} \times \text{CB}_-(m'_0, f_\sigma \sigma_-, f_{\alpha_-} \alpha_-, n) + (1 - f_{\text{low}}) \times \text{CB}_+(m'_0, f_\sigma \sigma_+, f_{\alpha_+} \alpha_+, n). \quad (2)$$

The CB functions each include a Gaussian component to describe the core of the mass distribution, as well as power-law tails to describe the radiative tail below (CB_-) and the non-Gaussian resolution above (CB_+) the signal peak. The extent of these tails is governed by the width and tail parameters, σ_\pm and α_\pm , respectively. The parameter m_0 is the fitted Λ_b^0 mass, and $m'_0 \equiv m_0 + \delta M$ is the Ξ_b^- mass, written in terms of the fitted mass difference, δM , between the two signals. The low-mass CB width, σ_- , is expressed in terms of the high-mass width using $\sigma_- = r_\sigma \sigma_+$. The parameters f_σ and f_{α_\pm} allow for possible differences in the mass resolutions and tail parameters, respectively, between the signal and normalization modes. We fix the power $n = 10$ and $f_{\text{low}} = 0.5$ to minimize the number of correlated parameters in the signal shape. The parameters r_σ , f_{α_+} , f_{α_-} , and f_σ are determined from simulated decays, and they are consistent with unity. These four parameters are fixed in fits to the data to the values from simulation, while σ_+ , α_+ and α_- are freely varied, along with m_0 and δM .

The invariant mass spectra also include partially reconstructed b -baryon background contributions, misidentified K^- in $X_b \rightarrow X_c K^-$ decays, as well as random track combinations, primarily from false X_c candidates. The main source of partially reconstructed background is from $X_b \rightarrow X_c \rho^-$ decays, where a π^0 from the ρ^- decay is not used to form the candidate. Its shape is obtained from simulated $\Lambda_b^0 \rightarrow \Lambda_c^+ \rho^-$ decays, and is assumed to be the same for both the signal and normalization modes, apart from a shift in the overall mass spectrum. A contribution from $\Lambda_b^0 \rightarrow \Sigma_c^+ \pi^-$, $\Sigma_c^+ \rightarrow \Lambda_c^+ \pi^0$ decays is also expected to populate the $\Lambda_c^+ \pi^-$ mass spectrum, and its shape is taken to be the same to that of the $\Lambda_b^0 \rightarrow \Lambda_c^+ \rho^-$ signal. An additional contribution from partially reconstructed Ξ_b decays is found, through a study of the Λ_c^+ sidebands, to populate the $\Lambda_c^+ \pi^-$ mass spectrum. This background is modeled through a fit to the Λ_b^0 candidate mass spectrum obtained using the lower and upper Λ_c^+ mass sidebands. The shape of the background from misidentified $X_b \rightarrow X_c K^-$ decays is taken from simulation. The misidentification rate of 3.1% is obtained from $D^{*+} \rightarrow D^0 \pi^+$ calibration samples, reweighted in p_T , η and number of tracks to match the distributions observed in data. No peaking contributions

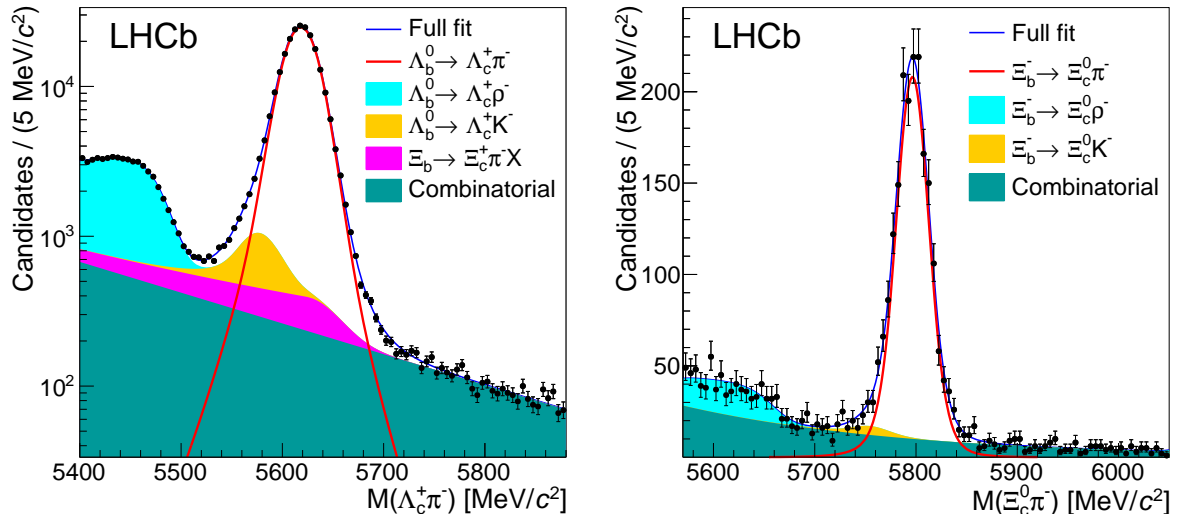


Figure 1: Invariant mass spectrum, along with the fit projections, for (left) $\Lambda_b^0 \rightarrow \Lambda_c^+ \pi^-$ and (right) $\Xi_b^- \rightarrow \Xi_c^0 \pi^-$ candidates.

from charmless backgrounds are observed when studying the X_b mass spectra using the X_c mass sidebands. The combinatorial background is modeled using an exponential function with a freely varying slope.

The $\Lambda_c^+ \pi^-$ and $\Xi_c^0 \pi^-$ mass spectra are fit simultaneously using a binned maximum likelihood fit. The results of the fit are shown in Fig. 1. A total of 1799 ± 46 $\Xi_b^- \rightarrow \Xi_c^0 \pi^-$ and $(220.0 \pm 0.5) \times 10^3$ $\Lambda_b^0 \rightarrow \Lambda_c^+ \pi^-$ signal decays are observed. The mass difference is measured to be

$$\delta M \equiv M(\Xi_b^-) - M(\Lambda_b^0) = 178.36 \pm 0.46 \text{ MeV}/c^2,$$

where the uncertainty is statistical only.

The observed signals are also used to measure the Ξ_b^- baryon lifetime relative to that of the Λ_b^0 baryon. We measure the efficiency-corrected yields in six bins of measured decay time, as given in Table 1. The ratio of efficiency-corrected yields depends exponentially on decay time as $N_{\text{cor}}[\Xi_b^- \rightarrow \Xi_c^0 \pi^-](t)/N_{\text{cor}}[\Lambda_b^0 \rightarrow \Lambda_c^+ \pi^-](t) = e^{\beta t}$, where $\beta = 1/\tau(\Lambda_b^0) - 1/\tau(\Xi_b^-)$. Many systematic uncertainties cancel to first order in the ratio, such as those associated with the time resolutions and relative acceptances.

The yields in each time bin are obtained using the results from the full fit with the signal shape parameters fixed. No dependence of the signal shapes on decay time is observed in simulated decays, as expected. The background shape parameters are also fixed, except for the combinatorial background shape parameter, and one of the $X_b \rightarrow X_c \rho$ shape parameters, which is seen to have a dependence on decay time. The signal yields in each of the time bins are shown in Table 1. The relative acceptance, shown in Fig. 2, is obtained using simulated decays after applying all event selection criteria. The efficiency for reconstructing the $\Xi_b^- \rightarrow \Xi_c^0 \pi^-$ mode is about a factor of two lower than that of

Table 1: Fitted yields of $\Lambda_b^0 \rightarrow \Lambda_c^+ \pi^-$ and $\Xi_b^- \rightarrow \Xi_c^0 \pi^-$ in each time bin. Uncertainties are statistical only.

Decay time (ps)	$\Lambda_b^0 \rightarrow \Lambda_c^+ \pi^-$	$\Xi_b^- \rightarrow \Xi_c^0 \pi^-$
0 – 1	$38,989 \pm 212$	260 ± 17
1 – 2	$79,402 \pm 299$	629 ± 27
2 – 3	$48,979 \pm 233$	436 ± 22
3 – 4	$26,010 \pm 169$	232 ± 16
4 – 6	$19,651 \pm 147$	177 ± 14
6 – 9	5794 ± 79	69 ± 9

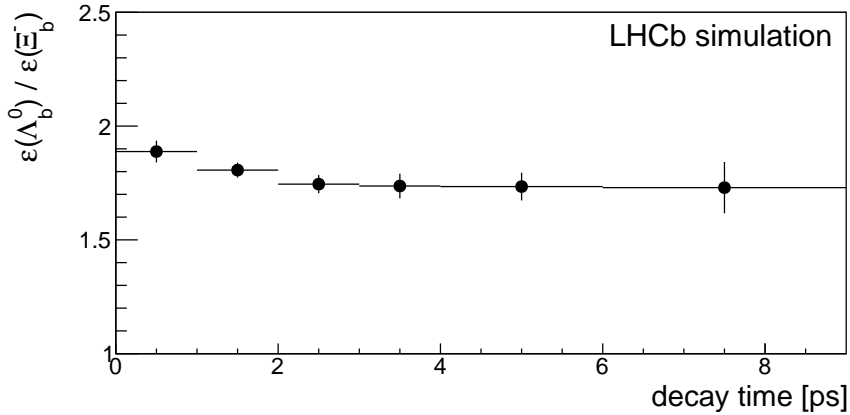


Figure 2: Ratio of the $\Lambda_b^0 \rightarrow \Lambda_c^+ \pi^-$ to the $\Xi_b^- \rightarrow \Xi_c^0 \pi^-$ selection efficiencies as a function of decay time. The uncertainties are due to the finite size of the simulated samples.

the $\Lambda_b^0 \rightarrow \Lambda_c^+ \pi^-$ decay due to the extra particle in the final state and the lower average momentum of the final-state particles. The relative efficiency, $\epsilon(\Lambda_b^0)/\epsilon(\Xi_b^-)$, is nearly uniform, with a gradual increase for decay times below 2 ps. This increase is expected, because the Λ_c^+ lifetime is about twice that of the Ξ_c^0 baryon, and the correspondingly larger impact parameters are favored by the software trigger and offline selections, most notably when the X_b decay time is small.

The ratios of corrected yields and the exponential fit are shown in Fig. 3. The points are displayed at the average time value in the bin assuming an exponential time distribution with mean 1.54 ps, which is the average of the known Λ_b^0 and fitted Ξ_b^- lifetimes. Choosing either the Λ_b^0 or the fitted Ξ_b^- lifetime leads to a negligible change in the result. The fitted value is $\beta = 0.0557 \pm 0.0160 \text{ ps}^{-1}$, where the uncertainty is statistical only. Using $\tau(\Lambda_b^0) = 1.468 \pm 0.009 \pm 0.008 \text{ ps}$ [43], we find

$$r_\tau \equiv \frac{\tau_{\Xi_b^-}}{\tau_{\Lambda_b^0}} = 1.089 \pm 0.026 \text{ (stat)}.$$

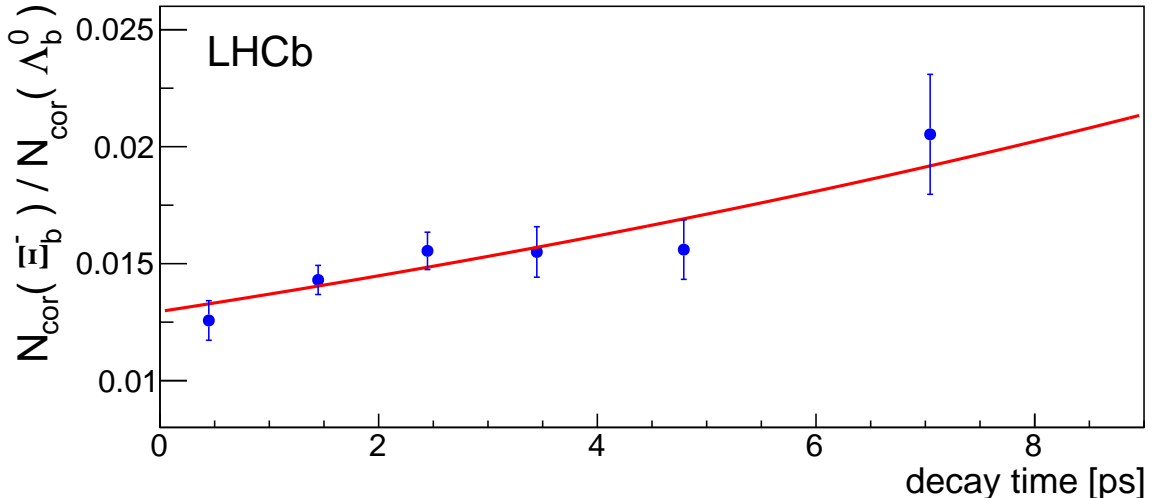


Figure 3: Corrected yield ratio, $N_{\text{cor}}(\Xi_b^-)/N_{\text{cor}}(\Lambda_b^0)$ in bins of decay time, along with the exponential fit. The uncertainties are statistical only.

Several consistency checks are performed, including comparing the mass differences obtained from 7 TeV versus 8 TeV data, opposite magnet polarities, X_b versus \bar{X}_b samples, and different trigger selections. In all cases, the results are consistent with statistical fluctuations of independent samples. In addition, the analysis is carried out using 15,500 $B^- \rightarrow D^0\pi^-$, $D^0 \rightarrow K^-K^+\pi^+\pi^-$ signal decays for normalization. The Ξ_b^- mass and lifetime results agree with the above values to better than one standard deviation, considering only the uncertainty due to the Λ_b^0 and B^- masses and lifetimes.

The measurements of $M(\Xi_b^-)$ and $\tau(\Xi_b^-)$ are subject to systematic uncertainties, but the largest contributions cancel to first order in δM and r_τ . For the mass difference measurement, the effect of the momentum scale uncertainty of 0.03% [44] is investigated by shifting the momenta of all final-state particles in simulated decays by this amount, leading to an uncertainty on δM of 0.08 MeV/ c^2 . Because the signal mode has one more particle than the normalization mode, the correction for energy loss in the detector material leads to an additional uncertainty of 0.06 MeV/ c^2 [44]. Uncertainty due to the signal modeling is 0.06 MeV/ c^2 , obtained by shifting all fixed parameters by their uncertainties, and adding the shifts in δM from the nominal value in quadrature. For the background model, several variations from the nominal fit are investigated, including (a) using a second-order polynomial to describe the combinatorial background, (b) allowing the fixed parameters in the partially reconstructed background to vary, (c) removing the Ξ_b background component, (d) a 20% relative increase in the $\Xi_b^- \rightarrow \Xi_c^0 K^-$ cross-feed, and (e) varying the fit range. The changes in δM are added in quadrature to obtain the background uncertainty of 0.11 MeV/ c^2 . Adding all sources of uncertainty in quadrature leads to a systematic uncertainty in δM of 0.16 MeV/ c^2 .

The largest source of systematic uncertainty in r_τ is the limited size of the simulated

samples, which contributes an uncertainty of 0.010. The simulated efficiencies are averaged over TOS and TIS events in the simulation, of which the former comprises 67% of the sample, compared to 57% in data. While the values of r_τ are statistically compatible between these two samples, if the efficiencies from simulation are reweighted to match the composition observed in data, a change in r_τ of 0.004 is found. This shift is assigned as a systematic uncertainty. Variation in the signal and background models lead to a negligible change in r_τ . We also consider possible different performances of the BDT in data versus simulation by correcting the data with an efficiency obtained with a tighter BDT requirement. The difference of 0.001 is assigned as a systematic uncertainty. For the proton efficiency, we use the values obtained from simulation. By varying the proton PID requirements, a maximal change of 0.001 is found, which is assigned as a systematic uncertainty. To investigate possible effects due to the larger Λ_c^+ lifetime (than the Ξ_c^0), we reject candidates with ct larger than 150 μm . The difference of 0.003 from the nominal result is assigned as a systematic uncertainty. In total, the systematic uncertainty on r_τ is 0.011.

In summary, we use a pp collision data sample corresponding to 3.0 fb^{-1} of integrated luminosity to improve the precision of the Ξ_b^- mass and lifetime by a factor of two over the previous best measurements. The resulting mass difference and relative lifetime are

$$\begin{aligned} M(\Xi_b^-) - M(\Lambda_b^0) &= 178.36 \pm 0.46 \pm 0.16 \text{ MeV}/c^2, \\ \frac{\tau_{\Xi_b^-}}{\tau_{\Lambda_b^0}} &= 1.089 \pm 0.026 \pm 0.011, \end{aligned}$$

where the uncertainties are statistical and systematic, respectively. Using the measured Λ_b^0 mass [45] and lifetime [43], we find

$$\begin{aligned} M(\Xi_b^-) &= 5797.72 \pm 0.46 \pm 0.16 \pm 0.26_{\Lambda_b^0} \text{ MeV}/c^2, \\ \tau_{\Xi_b^-} &= 1.599 \pm 0.041 \pm 0.018 \pm 0.012_{\Lambda_b^0} \text{ ps}, \end{aligned}$$

where the last uncertainty is due to the precision on the Λ_b^0 lifetime. Using the measurements of the Ξ_b^0 mass difference and relative lifetime, $M(\Xi_b^0) - M(\Lambda_b^0) = 172.44 \pm 0.39 \pm 0.17 \text{ MeV}/c^2$ and $\tau_{\Xi_b^0}/\tau_{\Lambda_b^0} = 1.006 \pm 0.018 \pm 0.010$ [15], we obtain

$$\begin{aligned} M(\Xi_b^-) - M(\Xi_b^0) &= 5.92 \pm 0.60 \pm 0.23 \text{ MeV}/c^2 \\ \frac{\tau_{\Xi_b^-}}{\tau_{\Xi_b^0}} &= 1.083 \pm 0.032 \pm 0.016. \end{aligned}$$

The measured isospin splitting between the Ξ_b^- and Ξ_b^0 baryons is consistent with the prediction in Ref. [22] of $6.24 \pm 0.21 \text{ MeV}/c^2$. The relative lifetime is 2.3 standard deviations larger than unity, giving a first indication that the Ξ_b^- baryon lifetime is larger than that of the Ξ_b^0 baryon. This result is consistent with the theoretical expectations of $\tau_{\Xi_b^-}/\tau_{\Xi_b^0} = 1.05 \pm 0.07$ [12] and $\tau_{\Xi_b^-}/\tau_{\Lambda_b^0} = 1.19^{+0.07}_{-0.06}$ [14], based on the HQE.

Acknowledgements

We express our gratitude to our colleagues in the CERN accelerator departments for the excellent performance of the LHC. We thank the technical and administrative staff at the LHCb institutes. We acknowledge support from CERN and from the national agencies: CAPES, CNPq, FAPERJ and FINEP (Brazil); NSFC (China); CNRS/IN2P3 (France); BMBF, DFG, HGF and MPG (Germany); SFI (Ireland); INFN (Italy); FOM and NWO (The Netherlands); MNiSW and NCN (Poland); MEN/IFA (Romania); MinES and FANO (Russia); MinECo (Spain); SNSF and SER (Switzerland); NASU (Ukraine); STFC (United Kingdom); NSF (USA). The Tier1 computing centres are supported by IN2P3 (France), KIT and BMBF (Germany), INFN (Italy), NWO and SURF (The Netherlands), PIC (Spain), GridPP (United Kingdom). We are indebted to the communities behind the multiple open source software packages on which we depend. We are also thankful for the computing resources and the access to software R&D tools provided by Yandex LLC (Russia). Individual groups or members have received support from EPLANET, Marie Skłodowska-Curie Actions and ERC (European Union), Conseil général de Haute-Savoie, Labex ENIGMASS and OCEVU, Région Auvergne (France), RFBR (Russia), XuntaGal and GENCAT (Spain), Royal Society and Royal Commission for the Exhibition of 1851 (United Kingdom).

References

- [1] V. A. Khoze and M. A. Shifman, *Heavy quarks*, Sov. Phys. Usp. **26** (1983) 387.
- [2] I. I. Bigi and N. G. Uraltsev, *Gluonic enhancements in non-spectator beauty decays - an inclusive mirage though an exclusive possibility*, Phys. Lett. **B280** (1992) 271.
- [3] I. I. Bigi, N. G. Uraltsev, and A. I. Vainshtein, *Nonperturbative corrections to inclusive beauty and charm decays. QCD versus phenomenological models*, Phys. Lett. **B293** (1992) 430, [arXiv:hep-ph/9207214](#).
- [4] B. Blok and M. Shifman, *The rule of discarding $1/N_c$ in inclusive weak decays (I)*, Nucl. Phys. **B399** (1993) 441, [arXiv:hep-ph/9207236](#).
- [5] B. Blok and M. Shifman, *The rule of discarding $1/N_c$ in inclusive weak decays (II)*, Nucl. Phys. **B399** (1993) 459, [arXiv:hep-ph/9209289](#).
- [6] M. Neubert, *B decays and the heavy quark expansion*, Adv. Ser. Direct. High Energy Phys. **15** (1998) 239, [arXiv:hep-ph/9702375](#).
- [7] N. Uraltsev, *Heavy quark expansion in beauty and its decays*, [arXiv:hep-ph/9804275](#), also published in proceedings, Heavy Flavour Physics: A Probe of Nature's Grand Design, Proc. Intern. School of Physics "Enrico Fermi", Course CXXXVII, Varenna, July 7-18 1997.

- [8] I. I. Bigi, *The QCD perspective on lifetimes of heavy flavor hadrons*, arXiv:hep-ph/9508408.
- [9] Particle Data Group, K. A. Olive *et al.*, *Review of particle physics*, Chin. Phys. **C38** (2014) 090001.
- [10] LHCb collaboration, R. Aaij *et al.*, *Measurement of the \bar{B}_s^0 meson lifetime in $D_s^+\pi^-$ decays*, Phys. Rev. Lett. **113** (2014) 172001, arXiv:1407.5873.
- [11] S. Stone, *Lifetimes of some b-flavored hadrons*, arXiv:1406.6497, Presented at 2014 Flavor Physics and CP Violation (FPCP-2014) Marseille, France, May 26-30, 2014, to appear in the proceedings.
- [12] A. Lenz, *Lifetimes and HQE*, arXiv:1405.3601, invited contribution to the Kolya Uraltsev Memorial Book.
- [13] K. G. Wilson, *Confinement of quarks*, Phys. Rev. **D10** (1974) 2445.
- [14] M. Voloshin, *Reducing model dependence of spectator effects in inclusive decays of heavy baryons*, Phys. Rev. **D61** (2000) 074026, arXiv:hep-ph/9908455.
- [15] LHCb collaboration, R. Aaij *et al.*, *Precision measurement of the mass and lifetime of the Ξ_b^0 baryon*, Phys. Rev. Lett. **113** (2014) 032001, arXiv:1405.7223.
- [16] LHCb collaboration, R. Aaij *et al.*, *Measurement of the Ξ_b^- and Ω_b^- baryon lifetimes*, Phys. Lett. **B736** (2014) 154, arXiv:1405.1543.
- [17] CDF collaboration, T. Aaltonen *et al.*, *Mass and lifetime measurements of bottom and charm baryons in $p\bar{p}$ collisions at $\sqrt{s} = 1.96$ TeV*, Phys. Rev. **D89** (2014) 072014, arXiv:1403.8126.
- [18] D. Ebert, R. N. Faustov, and V. O. Galkin, *Masses of heavy baryons in the relativistic quark model*, Phys. Rev. **D72** (2005) 034026, arXiv:hep-ph/0504112.
- [19] E. E. Jenkins, *Model-independent bottom baryon mass predictions in the $1/N_c$ expansion*, Phys. Rev. **D77** (2008) 034012, arXiv:0712.0406.
- [20] X. Liu *et al.*, *Bottom baryons*, Phys. Rev. **D77** (2008) 014031, arXiv:0710.0123.
- [21] R. Roncaglia, D. B. Lichtenberg, and E. Predazzi, *Predicting the masses of baryons containing one or two heavy quarks*, Phys. Rev. **D52** (1995) 1722, arXiv:hep-ph/9502251.
- [22] M. Karliner, B. Keren-Zur, H. J. Lipkin, and J. L. Rosner, *The quark model and b baryons*, Annals Phys. **324** (2009) 2, arXiv:0804.1575.
- [23] M. Karliner, *Heavy quark spectroscopy and prediction of bottom baryon masses*, Nucl. Phys. Proc. Suppl. **187** (2009) 21, arXiv:0806.4951.

- [24] W. Roberts and M. Pervin, *Heavy baryons in a quark model*, Int. J. Mod. Phys. **A23** (2008) 2817, [arXiv:0711.2492](#).
- [25] Z. Ghalehovi and A. Akbar Rajabi, *Single charm and beauty baryon masses in the hypercentral approach*, Eur. Phys. J. Plus **127** (2012) 141.
- [26] B. Patel, A. K. Rai, and P. C. Vinodkumar, *Masses and magnetic moments of heavy flavour baryons in hyper central model*, J. Phys. **G35** (2008) 065001, [arXiv:0710.3828](#).
- [27] B. Patel, A. K. Rai, and P. C. Vinodkumar, *Heavy flavour baryons in hyper central model*, Pramana **70** (2008) 797, [arXiv:0802.4408](#).
- [28] LHCb collaboration, R. Aaij *et al.*, *Measurements of the Λ_b^0 , Ξ_b^- , and Ω_b^- baryon masses*, Phys. Rev. Lett. **110** (2013) 182001, [arXiv:1302.1072](#).
- [29] LHCb collaboration, A. A. Alves Jr. *et al.*, *The LHCb detector at the LHC*, JINST **3** (2008) S08005.
- [30] M. Adinolfi *et al.*, *Performance of the LHCb RICH detector at the LHC*, Eur. Phys. J. **C73** (2013) 2431, [arXiv:1211.6759](#).
- [31] A. A. Alves Jr. *et al.*, *Performance of the LHCb muon system*, JINST **8** (2013) P02022, [arXiv:1211.1346](#).
- [32] R. Aaij *et al.*, *The LHCb trigger and its performance in 2011*, JINST **8** (2013) P04022, [arXiv:1211.3055](#).
- [33] V. V. Gligorov and M. Williams, *Efficient, reliable and fast high-level triggering using a bonsai boosted decision tree*, JINST **8** (2013) P02013, [arXiv:1210.6861](#).
- [34] T. Sjöstrand, S. Mrenna, and P. Skands, *PYTHIA 6.4 physics and manual*, JHEP **05** (2006) 026, [arXiv:hep-ph/0603175](#); T. Sjöstrand, S. Mrenna, and P. Skands, *A brief introduction to PYTHIA 8.1*, Comput. Phys. Commun. **178** (2008) 852, [arXiv:0710.3820](#).
- [35] I. Belyaev *et al.*, *Handling of the generation of primary events in GAUSS, the LHCb simulation framework*, Nuclear Science Symposium Conference Record (NSS/MIC) **IEEE** (2010) 1155.
- [36] D. J. Lange, *The EvtGen particle decay simulation package*, Nucl. Instrum. Meth. **A462** (2001) 152.
- [37] P. Golonka and Z. Was, *PHOTOS Monte Carlo: A precision tool for QED corrections in Z and W decays*, Eur. Phys. J. **C45** (2006) 97, [arXiv:hep-ph/0506026](#).

- [38] Geant4 collaboration, J. Allison *et al.*, *Geant4 developments and applications*, IEEE Trans. Nucl. Sci. **53** (2006) 270; Geant4 collaboration, S. Agostinelli *et al.*, *Geant4: a simulation toolkit*, Nucl. Instrum. Meth. **A506** (2003) 250.
- [39] M. Clemencic *et al.*, *The LHCb simulation application*, GAUSS: *Design, evolution and experience*, J. Phys. Conf. Ser. **331** (2011) 032023.
- [40] L. Breiman, J. H. Friedman, R. A. Olshen, and C. J. Stone, *Classification and regression trees*, Wadsworth international group, Belmont, California, USA, 1984.
- [41] Y. Freund and R. E. Schapire, *A decision-theoretic generalization of on-line learning and an application to boosting*, Jour. Comp. and Syst. Sc. **55** (1997) 119.
- [42] T. Skwarnicki, *A study of the radiative cascade transitions between the Upsilon-prime and Upsilon resonances*, PhD thesis, Institute of Nuclear Physics, Krakow, 1986, DESY-F31-86-02.
- [43] LHCb collaboration, R. Aaij *et al.*, *Precision measurement of the ratio of the Λ_b^0 to \bar{B}^0 lifetimes*, Phys. Lett. **B734** (2014) 122, [arXiv:1402.6242](#).
- [44] LHCb collaboration, R. Aaij *et al.*, *Precision measurement of D meson mass differences*, JHEP **06** (2013) 065, [arXiv:1304.6865](#).
- [45] LHCb collaboration, R. Aaij *et al.*, *Study of beauty hadron decays into pairs of charm hadrons*, Phys. Rev. Lett. **112** (2014) 202001, [arXiv:1403.3606](#).

LHCb collaboration

R. Aaij⁴¹, B. Adeva³⁷, M. Adinolfi⁴⁶, A. Affolder⁵², Z. Ajaltouni⁵, S. Akar⁶, J. Albrecht⁹, F. Alessio³⁸, M. Alexander⁵¹, S. Ali⁴¹, G. Alkhazov³⁰, P. Alvarez Cartelle³⁷, A.A. Alves Jr^{25,38}, S. Amato², S. Amerio²², Y. Amhis⁷, L. An³, L. Anderlini^{17,g}, J. Anderson⁴⁰, R. Andreassen⁵⁷, M. Andreotti^{16,f}, J.E. Andrews⁵⁸, R.B. Appleby⁵⁴, O. Aquines Gutierrez¹⁰, F. Archilli³⁸, A. Artamonov³⁵, M. Artuso⁵⁹, E. Aslanides⁶, G. Auriemma^{25,n}, M. Baalouch⁵, S. Bachmann¹¹, J.J. Back⁴⁸, A. Badalov³⁶, C. Baesso⁶⁰, W. Baldini¹⁶, R.J. Barlow⁵⁴, C. Barschel³⁸, S. Barsuk⁷, W. Barter⁴⁷, V. Batozskaya²⁸, V. Battista³⁹, A. Bay³⁹, L. Beaucourt⁴, J. Beddow⁵¹, F. Bedeschi²³, I. Bediaga¹, S. Belogurov³¹, K. Belous³⁵, I. Belyaev³¹, E. Ben-Haim⁸, G. Bencivenni¹⁸, S. Benson³⁸, J. Benton⁴⁶, A. Berezhnoy³², R. Bernet⁴⁰, M.-O. Bettler⁴⁷, M. van Beuzekom⁴¹, A. Bien¹¹, S. Bifani⁴⁵, T. Bird⁵⁴, A. Bizzeti^{17,i}, P.M. Bjørnstad⁵⁴, T. Blake⁴⁸, F. Blanc³⁹, J. Blouw¹⁰, S. Blusk⁵⁹, V. Bocci²⁵, A. Bondar³⁴, N. Bondar^{30,38}, W. Bonivento^{15,38}, S. Borghi⁵⁴, A. Borgia⁵⁹, M. Borsato⁷, T.J.V. Bowcock⁵², E. Bowen⁴⁰, C. Bozzi¹⁶, T. Brambach⁹, D. Brett⁵⁴, M. Britsch¹⁰, T. Britton⁵⁹, J. Brodzicka⁵⁴, N.H. Brook⁴⁶, H. Brown⁵², A. Bursche⁴⁰, J. Buytaert³⁸, S. Cadeddu¹⁵, R. Calabrese^{16,f}, M. Calvi^{20,k}, M. Calvo Gomez^{36,p}, P. Campana¹⁸, D. Campora Perez³⁸, A. Carbone^{14,d}, G. Carboni^{24,l}, R. Cardinale^{19,38,j}, A. Cardini¹⁵, L. Carson⁵⁰, K. Carvalho Akiba², G. Casse⁵², L. Cassina²⁰, L. Castillo Garcia³⁸, M. Cattaneo³⁸, Ch. Cauet⁹, R. Cenci²³, M. Charles⁸, Ph. Charpentier³⁸, M. Chefdeville⁴, S. Chen⁵⁴, S.-F. Cheung⁵⁵, N. Chiapolini⁴⁰, M. Chrzaszcz^{40,26}, X. Cid Vidal³⁸, G. Ciezarek⁵³, P.E.L. Clarke⁵⁰, M. Clemencic³⁸, H.V. Cliff⁴⁷, J. Closier³⁸, V. Coco³⁸, J. Cogan⁶, E. Cogneras⁵, V. Cogoni¹⁵, L. Cojocariu²⁹, G. Collazuol²², P. Collins³⁸, A. Comerma-Montells¹¹, A. Contu^{15,38}, A. Cook⁴⁶, M. Coombes⁴⁶, S. Coquereau⁸, G. Corti³⁸, M. Corvo^{16,f}, I. Counts⁵⁶, B. Couturier³⁸, G.A. Cowan⁵⁰, D.C. Craik⁴⁸, M. Cruz Torres⁶⁰, S. Cunliffe⁵³, R. Currie⁵³, C. D'Ambrosio³⁸, J. Dalseno⁴⁶, P. David⁸, P.N.Y. David⁴¹, A. Davis⁵⁷, K. De Bruyn⁴¹, S. De Capua⁵⁴, M. De Cian¹¹, J.M. De Miranda¹, L. De Paula², W. De Silva⁵⁷, P. De Simone¹⁸, C.-T. Dean⁵¹, D. Decamp⁴, M. Deckenhoff⁹, L. Del Buono⁸, N. Déleage⁴, D. Derkach⁵⁵, O. Deschamps⁵, F. Dettori³⁸, A. Di Canto³⁸, H. Dijkstra³⁸, S. Donleavy⁵², F. Dordei¹¹, M. Dorigo³⁹, A. Dosil Suárez³⁷, D. Dossett⁴⁸, A. Dovbnya⁴³, K. Dreimanis⁵², G. Dujany⁵⁴, F. Dupertuis³⁹, P. Durante³⁸, R. Dzhelyadin³⁵, A. Dziurda²⁶, A. Dzyuba³⁰, S. Easo^{49,38}, U. Egede⁵³, V. Egorychev³¹, S. Eidelman³⁴, S. Eisenhardt⁵⁰, U. Eitschberger⁹, R. Ekelhof⁹, L. Eklund⁵¹, I. El Rifai⁵, Ch. Elsasser⁴⁰, S. Ely⁵⁹, S. Esen¹¹, H.-M. Evans⁴⁷, T. Evans⁵⁵, A. Falabella¹⁴, C. Färber¹¹, C. Farinelli⁴¹, N. Farley⁴⁵, S. Farry⁵², R.F. Fay⁵², D. Ferguson⁵⁰, V. Fernandez Albor³⁷, F. Ferreira Rodrigues¹, M. Ferro-Luzzi³⁸, S. Filippov³³, M. Fiore^{16,f}, M. Fiorini^{16,f}, M. Firlej²⁷, C. Fitzpatrick³⁹, T. Fiutowski²⁷, P. Fol⁵³, M. Fontana¹⁰, F. Fontanelli^{19,j}, R. Forty³⁸, O. Francisco², M. Frank³⁸, C. Frei³⁸, M. Frosini^{17,g}, J. Fu^{21,38}, E. Furfaro^{24,l}, A. Gallas Torreira³⁷, D. Galli^{14,d}, S. Gallorini^{22,38}, S. Gambetta^{19,j}, M. Gandelman², P. Gandini⁵⁹, Y. Gao³, J. García Pardiñas³⁷, J. Garofoli⁵⁹, J. Garra Tico⁴⁷, L. Garrido³⁶, D. Gascon³⁶, C. Gaspar³⁸, R. Gauld⁵⁵, L. Gavardi⁹, A. Geraci^{21,v}, E. Gersabeck¹¹, M. Gersabeck⁵⁴, T. Gershon⁴⁸, Ph. Ghez⁴, A. Gianelle²², S. Gianì³⁹, V. Gibson⁴⁷, L. Giubega²⁹, V.V. Gligorov³⁸, C. Göbel⁶⁰, D. Golubkov³¹, A. Golutvin^{53,31,38}, A. Gomes^{1,a}, C. Gotti²⁰, M. Grabalosa Gándara⁵, R. Graciani Diaz³⁶, L.A. Granado Cardoso³⁸, E. Graugés³⁶, E. Graverini⁴⁰, G. Graziani¹⁷, A. Grecu²⁹, E. Greening⁵⁵, S. Gregson⁴⁷, P. Griffith⁴⁵, L. Grillo¹¹, O. Grünberg⁶³, B. Gui⁵⁹, E. Gushchin³³, Yu. Guz^{35,38}, T. Gys³⁸, C. Hadjivasiliou⁵⁹, G. Haefeli³⁹, C. Haen³⁸, S.C. Haines⁴⁷, S. Hall⁵³, B. Hamilton⁵⁸, T. Hampson⁴⁶, X. Han¹¹, S. Hansmann-Menzemer¹¹, N. Harnew⁵⁵, S.T. Harnew⁴⁶, J. Harrison⁵⁴, J. He³⁸, T. Head³⁸,

V. Heijne⁴¹, K. Hennessy⁵², P. Henrard⁵, L. Henry⁸, J.A. Hernando Morata³⁷,
 E. van Herwijnen³⁸, M. Heß⁶³, A. Hicheur², D. Hill⁵⁵, M. Hoballah⁵, C. Hombach⁵⁴,
 W. Hulsbergen⁴¹, P. Hunt⁵⁵, N. Hussain⁵⁵, D. Hutchcroft⁵², D. Hynds⁵¹, M. Idzik²⁷, P. Ilten⁵⁶,
 R. Jacobsson³⁸, A. Jaeger¹¹, J. Jalocha⁵⁵, E. Jans⁴¹, P. Jaton³⁹, A. Jawahery⁵⁸, F. Jing³,
 M. John⁵⁵, D. Johnson³⁸, C.R. Jones⁴⁷, C. Joram³⁸, B. Jost³⁸, N. Jurik⁵⁹, S. Kandybei⁴³,
 W. Kanso⁶, M. Karacson³⁸, T.M. Karbach³⁸, S. Karodia⁵¹, M. Kelsey⁵⁹, I.R. Kenyon⁴⁵,
 T. Ketel⁴², B. Khanji^{20,38}, C. Khurewathanakul³⁹, S. Klaver⁵⁴, K. Klimaszewski²⁸,
 O. Kochebina⁷, M. Kolpin¹¹, I. Komarov³⁹, R.F. Koopman⁴², P. Koppenburg^{41,38}, M. Korolev³²,
 A. Kozlinskiy⁴¹, L. Kravchuk³³, K. Kreplin¹¹, M. Kreps⁴⁸, G. Krocker¹¹, P. Krokovny³⁴,
 F. Kruse⁹, W. Kucewicz^{26,o}, M. Kucharczyk^{20,26,k}, V. Kudryavtsev³⁴, K. Kurek²⁸,
 T. Kvaratskheliya³¹, V.N. La Thi³⁹, D. Lacarrere³⁸, G. Lafferty⁵⁴, A. Lai¹⁵, D. Lambert⁵⁰,
 R.W. Lambert⁴², G. Lanfranchi¹⁸, C. Langenbruch⁴⁸, B. Langhans³⁸, T. Latham⁴⁸,
 C. Lazzeroni⁴⁵, R. Le Gac⁶, J. van Leerdam⁴¹, J.-P. Lees⁴, R. Lefèvre⁵, A. Leflat³²,
 J. Lefrançois⁷, S. Leo²³, O. Leroy⁶, T. Lesiak²⁶, B. Leverington¹¹, Y. Li³, T. Likhomanenko⁶⁴,
 M. Liles⁵², R. Lindner³⁸, C. Linn³⁸, F. Lionetto⁴⁰, B. Liu¹⁵, S. Lohn³⁸, I. Longstaff⁵¹,
 J.H. Lopes², N. Lopez-March³⁹, P. Lowdon⁴⁰, D. Lucchesi^{22,r}, H. Luo⁵⁰, A. Lupato²²,
 E. Luppi^{16,f}, O. Lupton⁵⁵, F. Machefert⁷, I.V. Machikhiliyan³¹, F. Maciuc²⁹, O. Maev³⁰,
 S. Malde⁵⁵, A. Malinin⁶⁴, G. Manca^{15,e}, G. Mancinelli⁶, A. Mapelli³⁸, J. Maratas⁵,
 J.F. Marchand⁴, U. Marconi¹⁴, C. Marin Benito³⁶, P. Marino^{23,t}, R. Märki³⁹, J. Marks¹¹,
 G. Martellotti²⁵, A. Martín Sánchez⁷, M. Martinelli³⁹, D. Martinez Santos^{42,38},
 F. Martinez Vidal⁶⁵, D. Martins Tostes², A. Massafferri¹, R. Matev³⁸, Z. Mathe³⁸,
 C. Matteuzzi²⁰, B. Maurin³⁹, A. Mazurov⁴⁵, M. McCann⁵³, J. McCarthy⁴⁵, A. McNab⁵⁴,
 R. McNulty¹², B. McSkelly⁵², B. Meadows⁵⁷, F. Meier⁹, M. Meissner¹¹, M. Merk⁴¹,
 D.A. Milanese⁶², M.-N. Minard⁴, N. Moggi¹⁴, J. Molina Rodriguez⁶⁰, S. Monteil⁵, M. Morandin²²,
 P. Morawski²⁷, A. Mordà⁶, M.J. Morello^{23,t}, J. Moron²⁷, A.-B. Morris⁵⁰, R. Mountain⁵⁹,
 F. Muheim⁵⁰, K. Müller⁴⁰, M. Mussini¹⁴, B. Muster³⁹, P. Naik⁴⁶, T. Nakada³⁹,
 R. Nandakumar⁴⁹, I. Nasteva², M. Needham⁵⁰, N. Neri²¹, S. Neubert³⁸, N. Neufeld³⁸,
 M. Neuner¹¹, A.D. Nguyen³⁹, T.D. Nguyen³⁹, C. Nguyen-Mau^{39,q}, M. Nicol⁷, V. Niess⁵,
 R. Niet⁹, N. Nikitin³², T. Nikodem¹¹, A. Novoselov³⁵, D.P. O'Hanlon⁴⁸,
 A. Oblakowska-Mucha^{27,38}, V. Obraztsov³⁵, S. Oggero⁴¹, S. Ogilvy⁵¹, O. Okhrimenko⁴⁴,
 R. Oldeman^{15,e}, C.J.G. Onderwater⁶⁶, M. Orlandea²⁹, J.M. Otalora Goicochea², A. Otto³⁸,
 P. Owen⁵³, A. Oyanguren⁶⁵, B.K. Pal⁵⁹, A. Palano^{13,c}, F. Palombo^{21,u}, M. Palutan¹⁸,
 J. Panman³⁸, A. Papanestis^{49,38}, M. Pappagallo⁵¹, L.L. Pappalardo^{16,f}, C. Parkes⁵⁴,
 C.J. Parkinson^{9,45}, G. Passaleva¹⁷, G.D. Patel⁵², M. Patel⁵³, C. Patrignani^{19,j}, A. Pearce⁵⁴,
 A. Pellegrino⁴¹, M. Pepe Altarelli³⁸, S. Perazzini^{14,d}, P. Perret⁵, M. Perrin-Terrin⁶,
 L. Pescatore⁴⁵, E. Pesen⁶⁷, K. Petridis⁵³, A. Petrolini^{19,j}, E. Picatoste Olloqui³⁶, B. Pietrzyk⁴,
 T. Pilar⁴⁸, D. Pinci²⁵, A. Pistone¹⁹, S. Playfer⁵⁰, M. Plo Casasus³⁷, F. Polci⁸, A. Poluektov^{48,34},
 E. Polcarpo², A. Popov³⁵, D. Popov¹⁰, B. Popovici²⁹, C. Potterat², E. Price⁴⁶, J.D. Price⁵²,
 J. Prisciandaro³⁹, A. Pritchard⁵², C. Prouve⁴⁶, V. Pugatch⁴⁴, A. Puig Navarro³⁹, G. Punzi^{23,s},
 W. Qian⁴, B. Rachwal²⁶, J.H. Rademacker⁴⁶, B. Rakotomiarmanana³⁹, M. Rama¹⁸,
 M.S. Rangel², I. Raniuk⁴³, N. Rauschmayr³⁸, G. Raven⁴², F. Redi⁵³, S. Reichert⁵⁴, M.M. Reid⁴⁸,
 A.C. dos Reis¹, S. Ricciardi⁴⁹, S. Richards⁴⁶, M. Rihl³⁸, K. Rinnert⁵², V. Rives Molina³⁶,
 P. Robbe⁷, A.B. Rodrigues¹, E. Rodrigues⁵⁴, P. Rodriguez Perez⁵⁴, S. Roiser³⁸,
 V. Romanovsky³⁵, A. Romero Vidal³⁷, M. Rotondo²², J. Rouvinet³⁹, T. Ruf³⁸, H. Ruiz³⁶,
 P. Ruiz Valls⁶⁵, J.J. Saborido Silva³⁷, N. Sagidova³⁰, P. Sail⁵¹, B. Saitta^{15,e},
 V. Salustino Guimaraes², C. Sanchez Mayordomo⁶⁵, B. Sanmartin Sedes³⁷, R. Santacesaria²⁵,

C. Santamarina Rios³⁷, E. Santovetti^{24,l}, A. Sarti^{18,m}, C. Satriano^{25,n}, A. Satta²⁴,
D.M. Saunders⁴⁶, D. Savrina^{31,32}, M. Schiller⁴², H. Schindler³⁸, M. Schlupp⁹, M. Schmelling¹⁰,
B. Schmidt³⁸, O. Schneider³⁹, A. Schopper³⁸, M. Schubiger³⁹, M.-H. Schune⁷, R. Schwemmer³⁸,
B. Sciascia¹⁸, A. Sciubba²⁵, A. Semennikov³¹, I. Sepp⁵³, N. Serra⁴⁰, J. Serrano⁶, L. Sestini²²,
P. Seyfert¹¹, M. Shapkin³⁵, I. Shapoval^{16,43,f}, Y. Shcheglov³⁰, T. Shears⁵², L. Shekhtman³⁴,
V. Shevchenko⁶⁴, A. Shires⁹, R. Silva Coutinho⁴⁸, G. Simi²², M. Sirendi⁴⁷, N. Skidmore⁴⁶,
I. Skillicorn⁵¹, T. Skwarnicki⁵⁹, N.A. Smith⁵², E. Smith^{55,49}, E. Smith⁵³, J. Smith⁴⁷, M. Smith⁵⁴,
H. Snoek⁴¹, M.D. Sokoloff⁵⁷, F.J.P. Soler⁵¹, F. Soomro³⁹, D. Souza⁴⁶, B. Souza De Paula²,
B. Spaan⁹, P. Spradlin⁵¹, S. Sridharan³⁸, F. Stagni³⁸, M. Stahl¹¹, S. Stahl¹¹, O. Steinkamp⁴⁰,
O. Stenyakin³⁵, S. Stevenson⁵⁵, S. Stoica²⁹, S. Stone⁵⁹, B. Storaci⁴⁰, S. Stracka²³,
M. Straticiu²⁹, U. Straumann⁴⁰, R. Stroili²², V.K. Subbiah³⁸, L. Sun⁵⁷, W. Sutcliffe⁵³,
K. Swientek²⁷, S. Swientek⁹, V. Syropoulos⁴², M. Szczekowski²⁸, P. Szczypka^{39,38}, T. Szumlak²⁷,
S. T'Jampens⁴, M. Teklishyn⁷, G. Tellarini^{16,f}, F. Teubert³⁸, C. Thomas⁵⁵, E. Thomas³⁸,
J. van Tilburg⁴¹, V. Tisserand⁴, M. Tobin³⁹, J. Todd⁵⁷, S. Tolk⁴², L. Tomassetti^{16,f},
D. Tonelli³⁸, S. Topp-Joergensen⁵⁵, N. Torr⁵⁵, E. Tournefier⁴, S. Tourneur³⁹, M.T. Tran³⁹,
M. Tresch⁴⁰, A. Trisovic³⁸, A. Tsaregorodtsev⁶, P. Tsopelas⁴¹, N. Tuning⁴¹, M. Ubeda Garcia³⁸,
A. Ukleja²⁸, A. Ustyuzhanin⁶⁴, U. Uwer¹¹, C. Vacca¹⁵, V. Vagnoni¹⁴, G. Valenti¹⁴, A. Vallier⁷,
R. Vazquez Gomez¹⁸, P. Vazquez Regueiro³⁷, C. Vázquez Sierra³⁷, S. Vecchi¹⁶, J.J. Velthuis⁴⁶,
M. Veltri^{17,h}, G. Veneziano³⁹, M. Vesterinen¹¹, B. Viaud⁷, D. Vieira², M. Vieites Diaz³⁷,
X. Vilasis-Cardona^{36,p}, A. Vollhardt⁴⁰, D. Volyanskyy¹⁰, D. Voong⁴⁶, A. Vorobyev³⁰,
V. Vorobyev³⁴, C. Voß⁶³, J.A. de Vries⁴¹, R. Waldi⁶³, C. Wallace⁴⁸, R. Wallace¹², J. Walsh²³,
S. Wandernoth¹¹, J. Wang⁵⁹, D.R. Ward⁴⁷, N.K. Watson⁴⁵, D. Websdale⁵³, M. Whitehead⁴⁸,
J. Wicht³⁸, D. Wiedner¹¹, G. Wilkinson^{55,38}, M.P. Williams⁴⁵, M. Williams⁵⁶, H.W. Wilschut⁶⁶,
F.F. Wilson⁴⁹, J. Wimberley⁵⁸, J. Wishahi⁹, W. Wislicki²⁸, M. Witek²⁶, G. Wormser⁷,
S.A. Wotton⁴⁷, S. Wright⁴⁷, K. Wyllie³⁸, Y. Xie⁶¹, Z. Xing⁵⁹, Z. Xu³⁹, Z. Yang³, X. Yuan³,
O. Yushchenko³⁵, M. Zangoli¹⁴, M. Zavertyaev^{10,b}, L. Zhang⁵⁹, W.C. Zhang¹², Y. Zhang³,
A. Zhelezov¹¹, A. Zhokhov³¹, L. Zhong³.

¹ Centro Brasileiro de Pesquisas Físicas (CBPF), Rio de Janeiro, Brazil

² Universidade Federal do Rio de Janeiro (UFRJ), Rio de Janeiro, Brazil

³ Center for High Energy Physics, Tsinghua University, Beijing, China

⁴ LAPP, Université de Savoie, CNRS/IN2P3, Annecy-Le-Vieux, France

⁵ Clermont Université, Université Blaise Pascal, CNRS/IN2P3, LPC, Clermont-Ferrand, France

⁶ CPPM, Aix-Marseille Université, CNRS/IN2P3, Marseille, France

⁷ LAL, Université Paris-Sud, CNRS/IN2P3, Orsay, France

⁸ LPNHE, Université Pierre et Marie Curie, Université Paris Diderot, CNRS/IN2P3, Paris, France

⁹ Fakultät Physik, Technische Universität Dortmund, Dortmund, Germany

¹⁰ Max-Planck-Institut für Kernphysik (MPIK), Heidelberg, Germany

¹¹ Physikalisches Institut, Ruprecht-Karls-Universität Heidelberg, Heidelberg, Germany

¹² School of Physics, University College Dublin, Dublin, Ireland

¹³ Sezione INFN di Bari, Bari, Italy

¹⁴ Sezione INFN di Bologna, Bologna, Italy

¹⁵ Sezione INFN di Cagliari, Cagliari, Italy

¹⁶ Sezione INFN di Ferrara, Ferrara, Italy

¹⁷ Sezione INFN di Firenze, Firenze, Italy

¹⁸ Laboratori Nazionali dell'INFN di Frascati, Frascati, Italy

¹⁹ Sezione INFN di Genova, Genova, Italy

²⁰ Sezione INFN di Milano Bicocca, Milano, Italy

²¹ Sezione INFN di Milano, Milano, Italy

- ²² *Sezione INFN di Padova, Padova, Italy*
- ²³ *Sezione INFN di Pisa, Pisa, Italy*
- ²⁴ *Sezione INFN di Roma Tor Vergata, Roma, Italy*
- ²⁵ *Sezione INFN di Roma La Sapienza, Roma, Italy*
- ²⁶ *Henryk Niewodniczanski Institute of Nuclear Physics Polish Academy of Sciences, Kraków, Poland*
- ²⁷ *AGH - University of Science and Technology, Faculty of Physics and Applied Computer Science, Kraków, Poland*
- ²⁸ *National Center for Nuclear Research (NCBJ), Warsaw, Poland*
- ²⁹ *Horia Hulubei National Institute of Physics and Nuclear Engineering, Bucharest-Magurele, Romania*
- ³⁰ *Petersburg Nuclear Physics Institute (PNPI), Gatchina, Russia*
- ³¹ *Institute of Theoretical and Experimental Physics (ITEP), Moscow, Russia*
- ³² *Institute of Nuclear Physics, Moscow State University (SINP MSU), Moscow, Russia*
- ³³ *Institute for Nuclear Research of the Russian Academy of Sciences (INR RAN), Moscow, Russia*
- ³⁴ *Budker Institute of Nuclear Physics (SB RAS) and Novosibirsk State University, Novosibirsk, Russia*
- ³⁵ *Institute for High Energy Physics (IHEP), Protvino, Russia*
- ³⁶ *Universitat de Barcelona, Barcelona, Spain*
- ³⁷ *Universidad de Santiago de Compostela, Santiago de Compostela, Spain*
- ³⁸ *European Organization for Nuclear Research (CERN), Geneva, Switzerland*
- ³⁹ *Ecole Polytechnique Fédérale de Lausanne (EPFL), Lausanne, Switzerland*
- ⁴⁰ *Physik-Institut, Universität Zürich, Zürich, Switzerland*
- ⁴¹ *Nikhef National Institute for Subatomic Physics, Amsterdam, The Netherlands*
- ⁴² *Nikhef National Institute for Subatomic Physics and VU University Amsterdam, Amsterdam, The Netherlands*
- ⁴³ *NSC Kharkiv Institute of Physics and Technology (NSC KIPT), Kharkiv, Ukraine*
- ⁴⁴ *Institute for Nuclear Research of the National Academy of Sciences (KINR), Kyiv, Ukraine*
- ⁴⁵ *University of Birmingham, Birmingham, United Kingdom*
- ⁴⁶ *H.H. Wills Physics Laboratory, University of Bristol, Bristol, United Kingdom*
- ⁴⁷ *Cavendish Laboratory, University of Cambridge, Cambridge, United Kingdom*
- ⁴⁸ *Department of Physics, University of Warwick, Coventry, United Kingdom*
- ⁴⁹ *STFC Rutherford Appleton Laboratory, Didcot, United Kingdom*
- ⁵⁰ *School of Physics and Astronomy, University of Edinburgh, Edinburgh, United Kingdom*
- ⁵¹ *School of Physics and Astronomy, University of Glasgow, Glasgow, United Kingdom*
- ⁵² *Oliver Lodge Laboratory, University of Liverpool, Liverpool, United Kingdom*
- ⁵³ *Imperial College London, London, United Kingdom*
- ⁵⁴ *School of Physics and Astronomy, University of Manchester, Manchester, United Kingdom*
- ⁵⁵ *Department of Physics, University of Oxford, Oxford, United Kingdom*
- ⁵⁶ *Massachusetts Institute of Technology, Cambridge, MA, United States*
- ⁵⁷ *University of Cincinnati, Cincinnati, OH, United States*
- ⁵⁸ *University of Maryland, College Park, MD, United States*
- ⁵⁹ *Syracuse University, Syracuse, NY, United States*
- ⁶⁰ *Pontifícia Universidade Católica do Rio de Janeiro (PUC-Rio), Rio de Janeiro, Brazil, associated to ²*
- ⁶¹ *Institute of Particle Physics, Central China Normal University, Wuhan, Hubei, China, associated to ³*
- ⁶² *Departamento de Física, Universidad Nacional de Colombia, Bogota, Colombia, associated to ⁸*
- ⁶³ *Institut für Physik, Universität Rostock, Rostock, Germany, associated to ¹¹*
- ⁶⁴ *National Research Centre Kurchatov Institute, Moscow, Russia, associated to ³¹*
- ⁶⁵ *Instituto de Física Corpuscular (IFIC), Universitat de Valencia-CSIC, Valencia, Spain, associated to ³⁶*
- ⁶⁶ *Van Swinderen Institute, University of Groningen, Groningen, The Netherlands, associated to ⁴¹*
- ⁶⁷ *Celal Bayar University, Manisa, Turkey, associated to ³⁸*

^a *Universidade Federal do Triângulo Mineiro (UFMT), Uberaba-MG, Brazil*

^b *P.N. Lebedev Physical Institute, Russian Academy of Science (LPI RAS), Moscow, Russia*

^c *Università di Bari, Bari, Italy*

- ^d *Università di Bologna, Bologna, Italy*
^e *Università di Cagliari, Cagliari, Italy*
^f *Università di Ferrara, Ferrara, Italy*
^g *Università di Firenze, Firenze, Italy*
^h *Università di Urbino, Urbino, Italy*
ⁱ *Università di Modena e Reggio Emilia, Modena, Italy*
^j *Università di Genova, Genova, Italy*
^k *Università di Milano Bicocca, Milano, Italy*
^l *Università di Roma Tor Vergata, Roma, Italy*
^m *Università di Roma La Sapienza, Roma, Italy*
ⁿ *Università della Basilicata, Potenza, Italy*
^o *AGH - University of Science and Technology, Faculty of Computer Science, Electronics and Telecommunications, Kraków, Poland*
^p *LIFAELS, La Salle, Universitat Ramon Llull, Barcelona, Spain*
^q *Hanoi University of Science, Hanoi, Viet Nam*
^r *Università di Padova, Padova, Italy*
^s *Università di Pisa, Pisa, Italy*
^t *Scuola Normale Superiore, Pisa, Italy*
^u *Università degli Studi di Milano, Milano, Italy*
^v *Politecnico di Milano, Milano, Italy*